

Fair load-side control for frequency regulation in smart grids

Enrique Mallada, *Member, IEEE*, Changhong Zhao, *Student Member, IEEE*, and Steven Low, *Fellow, IEEE*

Abstract—Frequency control rebalances supply and demand while maintaining the network state within operational margins. It is implemented using fast ramping reserves that are expensive and non-renewable, and which are expected to grow with the increasing penetration of renewables. The most promising solution to this problem is the use of demand response, i.e. load participation in frequency control. Yet it is still unclear how to efficiently integrate load participation without introducing instabilities and violating operational constraints.

In this paper we present a comprehensive load-side frequency control mechanism that can maintain the grid within operational constraints. Our controllers can rebalance supply and demand after disturbances, restore the frequency to its nominal value and preserve inter-area power flows. Furthermore, our controllers are distributed (unlike generation-side), fair among participating loads, and can further maintain line flows within thermal limits. We prove that such a distributed load-side control is globally asymptotically stable and illustrate its convergence with simulation.

I. INTRODUCTION

Frequency control maintains the frequency of a power network at its nominal value when demand or supply fluctuates. It is traditionally implemented on the generation side and consists of three mechanisms that work in concert [1]–[3]. The primary frequency control, called the droop control and completely decentralized, operates on a timescale up to low tens of seconds and uses a governor to adjust, around a setpoint, the mechanical power input to a generator based on the local frequency deviation. The primary control can rebalance power and stabilize the frequency but does not restore the nominal frequency. The secondary frequency control (called automatic generation control) operates on a timescale up to a minute or so and adjusts the setpoints of governors in a control area in a centralized fashion to drive the frequency back to its nominal value and the inter-area power flows to their scheduled values. Economic dispatch operates on a timescale of several minutes or up and schedules the output levels of generators that are online and the inter-area power flows. See [4], [5] for a recent hierarchical model of power systems and their stability analysis.

Load-side participation in frequency control offers many advantages, including faster response, lower fuel consumption and emission, and better localization of disturbances. The idea of using frequency adaptive loads dates back to [6] that advocates their large scale deployment to “assist or even replace turbine-governed systems and spinning reserve.”

The authors are with the Department of Computational and Mathematical Sciences, California Institute of Technology, Pasadena, CA 91125 USA (e-mail: {mallada,czhao,slow}@caltech.edu).

This work was supported by NSF NetSE grant CNS 0911041, ARPA-E grant DE-AR0000226, Southern California Edison, National Science Council of Taiwan R.O.C. grant NSC 103-3113-P-008-001, and Caltech Resnick Institute.

They also proposed to use spot prices to incentivize the users to adapt their consumption to the true cost of generation at the time of consumption. Remarkably it was emphasized back then that such frequency adaptive loads will “allow the system to accept more readily a stochastically fluctuating energy source, such as wind or solar generation” [6]. This is echoed recently in, e.g., [7]–[13] that argue for “grid-friendly” appliances, such as refrigerators, water or space heaters, ventilation systems, and air conditioners, as well as plug-in electric vehicles to help manage energy imbalance. Simulations in all these studies have consistently shown significant improvement in performance and reduction in the need for spinning reserves. A small scale project by the Pacific Northwest National Lab in 2006–2007 demonstrated the use of 200 residential appliances in primary frequency control that automatically reduce their consumption when the frequency of the household dropped below a threshold (59.95Hz) [14].

Despite these simulation studies and field trials, there has not been much analytic study of how large-scale deployment of distributed frequency control will behave until very recently. Some notable examples include the works on distributed secondary frequency control in power systems [5], [15]–[17] and microgrids [18]–[22]. However, it is yet to be designed a general solution that can rebalance supply and demand, restore nominal frequency, preserve inter-area flows and avoid thermal limits violations.

Recently another model is presented in [23] that formulates an optimal load control (OLC) problem where the objective is to minimize the aggregate disutility of tracking an operating point subject to power balance over the network. The main conclusion is that decentralized load-side primary frequency control, coupled with the power network dynamics, serves as a primal-dual algorithm to solve (the Lagrangian dual of) OLC. Like the droop control on the generation side, the scheme in [23] rebalances power and resynchronizes frequencies after a disturbance, but does not drive the system to a desirable operating point. Similar ideas since then has then been developed to include AGC and governor dynamics [24] and to use load-side secondary frequency control to restore the frequency to its nominal value [25].

In this paper, we extend this framework to allow the system restore the desired operational constraints. We first modify the OLC problem to include the operational constraints in Section III. The crux of our contribution is the introduction of surrogate line flows that in equilibrium are equal to the real line flows. This allows to derive a distributed solution that preserves the primal-dual interpretation of the

network dynamics (Section IV). We prove that our design is globally asymptotically stable and converges to an optimal solution of the modified OLC (Section V). Finally we present simulations to illustrate these results (Section VI).

II. PRELIMINARIES

Let \mathbb{R} be the set of real numbers and \mathbb{N} the set of natural numbers. Given a finite set $S \subset \mathbb{N}$ we use $|S|$ to denote its cardinality. For a set of scalar numbers $a_i \in \mathbb{R}$, $i \in S$, we denote a_S as the column vector of the a_i components, i.e. $a_S := (a_i, i \in S) \in \mathbb{R}^{|S|}$; we usually drop the subscript S when the set is known from the context. Similarly, for two vectors $a \in \mathbb{R}^{|S|}$ and $b \in \mathbb{R}^{|S'|}$ we define the column vector $x = (a, b) \in \mathbb{R}^{|S|+|S'|}$. Given any matrix A , we denote its transpose as A^T and use A_i to denote the i th row of A . We will also use A_S to denote the sub matrix of A composed only of the rows A_i with $i \in S$. The diagonal matrix of a sequence $\{a_i, i \in S\}$, is represented by $\text{diag}(a_i)_{i \in S}$. Similarly, for a sequence of matrices $\{A_h, h \in S\}$ we let $\text{blockdiag}(A_h)_{h \in S}$ denote the block diagonal matrix. Finally, we use $\mathbf{1}$ ($\mathbf{0}$) to denote the vector of all ones (zeros).

A. Network Model

We consider a power network described by a directed graph $G(\mathcal{N}, \mathcal{E})$ where $\mathcal{N} = \{1, \dots, |\mathcal{N}|\}$ is the set of buses and $\mathcal{E} \subset \mathcal{N} \times \mathcal{N}$ is the set of transmission lines denoted by either e or ij such that if $ij \in \mathcal{E}$, then $ji \notin \mathcal{E}$. We partition the buses $\mathcal{N} = \mathcal{G} \cup \mathcal{L}$ and use \mathcal{G} and \mathcal{L} to denote the set of generator and load buses respectively.

The evolution of the transmission network is described by

$$M_i \dot{\omega}_i = P_i^m - (d_i + \hat{d}_i) - \sum_{e \in \mathcal{E}} C_{i,e} P_e \quad i \in \mathcal{G} \quad (1a)$$

$$0 = P_i^m - (d_i + \hat{d}_i) - \sum_{e \in \mathcal{E}} C_{i,e} P_e \quad i \in \mathcal{L} \quad (1b)$$

$$\dot{P}_{ij} = B_{ij}(\omega_i - \omega_j) \quad ij \in \mathcal{E} \quad (1c)$$

$$\hat{d}_i = D_i \omega_i \quad i \in \mathcal{N} \quad (1d)$$

where d_i denotes an aggregate controllable load, \hat{d}_i denotes an aggregate uncontrollable but frequency-sensitive load as well as damping loss at generator i , M_i is the generator's inertia, P_i^m is the mechanical power injected by a generator $i \in \mathcal{G}$, $-P_i^m$ is the aggregate power consumed by constant loads for $i \in \mathcal{L}$, and P_{ij} is the line real power flow from i to j . Finally, $C_{i,e}$ are the elements of the incidence matrix $C \in \mathbb{R}^{|\mathcal{N}| \times |\mathcal{E}|}$ of the graph $G(\mathcal{N}, \mathcal{E})$ such that $C_{i,e} = -1$ if $e = ji \in \mathcal{E}$, $C_{i,e} = 1$ if $e = ij \in \mathcal{E}$ and $C_{i,e} = 0$ otherwise.

Equation (1) describes the evolution of the frequency and line flows when their values are close to schedule values P_{ij}^0 and ω^0 . In other words, $P_{ij} = P_{ij}^0 + \delta P_{ij}$ and $\omega_i = \omega_0 + \delta \omega_i$ with δP_{ij} and $\delta \omega_i$ small enough. We also assume purely inductive lines as well as the standard *decoupling approximation* [26]. However, the analysis can be extended to networks with constant R/X ratio [27]. We refer the reader to [28] for a detailed motivation of the model.

For notational convenience we will use whenever needed the vector form of (1), i.e.

$$\begin{aligned} M_G \dot{\omega}_G &= P_G^m - (d_G + \hat{d}_G) - C_G P \\ 0 &= P_L^m - (d_L + \hat{d}_L) - C_L P \\ \dot{P} &= D_B C^T \omega \\ \hat{d} &= D \omega \end{aligned}$$

where the matrices C_L and C_G are defined by splitting the the rows of C between generator and load buses, i.e. $C = [C_G^T \ C_L^T]^T$, $D = \text{diag}(D_i)_{i \in \mathcal{N}}$, $D_B = \text{diag}(B_{ij})_{ij \in \mathcal{E}}$ and $M_G = \text{diag}(M_i)_{i \in \mathcal{G}}$

B. Operational Constraints

We denote each control area using either k or l , and let $\mathcal{K} := \{1, \dots, |\mathcal{K}|\}$ denote the set of areas. Within each area, the Automatic Generation Control (AGC) scheme seeks to balance supply and demand, while keeping the frequency to its nominal value as well as preserving a constant power transfer outside the area, i.e.

$$\sum_{i \in \mathcal{N}_k} \sum_{e \in \mathcal{E}} C_{i,e} P_e = e_k^T C P = \hat{P}_k, \quad \forall k \in \mathcal{K}, \quad (2)$$

where $\mathcal{N}_k \subset \mathcal{N}$ is the set of buses of area $k \in \mathcal{K}$, $e_k \in \mathbb{R}^{|\mathcal{N}|}$, $k \in \mathcal{K}$, is a vector with elements $(e_k)_i = 1$ if $i \in \mathcal{N}_k$ and $(e_k)_i = 0$ otherwise, \hat{P}_k is the net scheduled power injection of area k .

Notice that if we define

$$\hat{C}^b := E_{\mathcal{K}} C \quad (3)$$

with $E_{\mathcal{K}} := [e_1 \ \dots \ e_{|\mathcal{K}|}]^T$ and $\hat{C}^b \in \mathbb{R}^{|\mathcal{K}| \times |\mathcal{E}|}$, then constraint (2) can be compactly expressed using

$$\hat{C}^b P = \hat{P} \quad (4)$$

where $\hat{P} = (\hat{P}_k)_{k \in \mathcal{K}}$. It is easy to see that $\hat{C}_{k,e}^b$ ($e = ij$) is equal to 1 if ij is an inter-area line with $i \in \mathcal{N}_k$, -1 if ij is an inter-area line with $j \in \mathcal{N}_k$, and 0 otherwise.

Finally, the thermal limit constraints are usually given by

$$\underline{P} \leq P \leq \bar{P} \quad (5)$$

where $\bar{P} := (\bar{P}_e)_{e \in \mathcal{E}}$ and $\underline{P} := (\underline{P}_e)_{e \in \mathcal{E}}$ represent the line flow limits; usually $\underline{P} = -\bar{P}$ so that we get $|P| \leq \bar{P}$.

C. Fair Load Control

Suppose the system (1) is in equilibrium, i.e. $\dot{\omega}_i = 0$ for all i and $\dot{P}_{ij} = 0$ for all ij , and at time 0, there is a disturbance represented by the vector (perturbations) $P^m := (P_i^m, i \in \mathcal{G} \cup \mathcal{L})$ that produces a power imbalance. Then, we are interested in designing a distributed control mechanism that rebalances the system while preserving the frequency in its nominal value as well as maintaining the scheduled power transfer between areas. Furthermore, we would like this mechanism to be fair among all the users (or loads) that are willing to adapt and to impose thermal limit constraints.

We use $c_i(d_i)$ and $\frac{d_i^2}{2D_i}$ to denote the cost or disutility of changing the load consumption by d_i and \hat{d}_i respectively.

This allows us to formally describe our notion of fairness in terms of the loads' welfare. More precisely, we shall say that a load control (d, \hat{d}) is fair if it solves the following problem.

Problem 1 (WELFARE):

$$\underset{d, \hat{d}}{\text{minimize}} \quad \sum_{i \in \mathcal{N}} c_i(d_i) + \frac{\hat{d}_i^2}{2D_i} \quad (6)$$

subject to operational constraints.

Problem 1 has been originally proposed in [28] for the case where the operational constraint is to balance supply and demand, i.e.

$$\sum_{i \in \mathcal{N}} (d_i + \hat{d}_i) = \sum_{i \in \mathcal{N}} P_i^m. \quad (7)$$

It is shown in [28] that when

$$d_i = c_i'^{-1}(\omega_i), \quad (8)$$

then (1) is a distributed primal-dual algorithm that solves (6) subject to (7).

Therefore, one can use problem (6)-(7) to forward engineer the desired controllers, by means of primal-dual decomposition, that can rebalance supply and demand. Unfortunately, system (1) and (8) suffers from the disadvantage that the optimal solution of (6)-(7) may not satisfy the additional operational constraints described in Section II-B.

In the next section we shall see that a clever modification of (6)-(7) will be able to restore the nominal frequency while maintaining the interpretation of (1) as a *component* of the primal-dual algorithm that solves the modified optimization problem. An additional byproduct of the formulation is that we can also impose any type of linear equality and inequality constraint that the operator may require.

III. OPTIMAL LOAD-SIDE INTRA AREA CONTROL

We now proceed to describe the optimization problem that will be used to derive the distributed controllers that achieve our goals. The crux of our solution comes from including additional constraints to Problem 1 that implicitly guarantee the desired operational constraints, yet still preserves the desired structure which allows the use of (1) as part of the optimization algorithm.

Thus, we will use the following modified version of Problem 1 called Optimal Load-side Frequency Control (OLFC)

Problem 2 (OLFC):

$$\underset{d, \hat{d}, P, v}{\text{minimize}} \quad \sum_{i \in \mathcal{N}} c_i(d_i) + \frac{\hat{d}_i^2}{2D_i} \quad (9a)$$

subject to

$$P^m - (d + \hat{d}) = CP \quad (9b)$$

$$P^m - d = L_a v \quad (9c)$$

$$\hat{C}^b D_a C^T v = \hat{P} \quad (9d)$$

$$\underline{P} \leq D_a C^T v \leq \bar{P} \quad (9e)$$

where $D_a := \text{diag}(a_{ij})_{ij \in \mathcal{E}}$, $L_a := CD_a C^T$ is the a_e -weighted Laplacian matrix and a_{ij} , $ij \in \mathcal{E}$, are some positive weights whose values will be defined later.

Although not clear at first sight, the constraint (9c) implicitly enforces that any optimal solution of OLFC $(d^*, \hat{d}^*, P^*, v^*)$ will restore the frequency to its nominal value, i.e. $\hat{d}_i^* = D_i \omega^* = 0$. Similarly, we will use constraint (9d) to impose (2) (or equivalently (4)) and (9e) to impose (5).

Throughout this paper we make the following assumptions:

Assumption 1 (Cost function): The cost function $c_i(d_i)$ is α -strongly convex and second order differentiable ($c_i \in C^2$ with $c_i''(d_i) \geq \alpha > 0$) in the interior of its domain $\mathcal{D}_i := [\underline{d}_i, \bar{d}_i] \subseteq \mathbb{R}$, such that $c_i(d_i) \rightarrow +\infty$ whenever $d_i \rightarrow \partial \mathcal{D}_i$.

Assumption 2 (Slater Condition): The OLFC problem (9) is feasible [29, Ch. 5.2.3].

The remainder of this section is devoted to understanding the properties of the optimal solutions of OLFC. We will use ν_i , λ_i and π_k as Lagrange multipliers of constraints (9b), (9c) and (9d), and ρ_{ij}^+ and ρ_{ij}^- as multipliers of the right and left constraints of (9e), respectively. In order to make the presentation more compact sometimes we will use $x = (P, v) \in \mathbb{R}^{|\mathcal{E}|+|\mathcal{N}|}$ and $\sigma = (\nu, \lambda, \pi, \rho^+, \rho^-) \in \mathbb{R}^{2|\mathcal{N}|+|\mathcal{E}|+2|\mathcal{E}|}$, as well as $\sigma_i = (\nu_i, \lambda_i)$, $\sigma_k = (\pi_k)$ and $\sigma_{ij} = (\rho_{ij}^+, \rho_{ij}^-)$. We will also use $\rho := (\rho^+, \rho^-)$.

Next, we consider the dual function $D(\sigma)$ of the OLFC problem.

$$D(\sigma) = \inf_{d, \hat{d}, x} L(d, \hat{d}, x, \sigma) \quad (10)$$

where

$$\begin{aligned} L(d, \hat{d}, x, \sigma) &= \sum_{i \in \mathcal{N}} (c_i(d_i) + \frac{\hat{d}_i^2}{2D_i}) + \nu^T (P^m - (d + \hat{d}) \\ &\quad - CP) + \lambda^T (P^m - d - L_a v) + \pi^T (\hat{C}^b D_a C^T v - \hat{P}) \\ &\quad + \rho^{+T} (D_a C^T v - \bar{P}) + \rho^{-T} (\underline{P} - D_a C^T v) \\ &= \sum_{i \in \mathcal{N}} (c_i(d_i) - (\lambda_i + \nu_i) d_i + \frac{\hat{d}_i^2}{2D_i} - \nu_i \hat{d}_i + (\nu_i + \lambda_i) P_i^m) \\ &\quad - P^T C^T \nu - v^T (L_a \lambda - CD_a \hat{C}^{bT} \pi - CD_a (\rho^+ - \rho^-)) \\ &\quad - \pi^T \hat{P} - \rho^{+T} \bar{P} + \rho^{-T} \underline{P} \end{aligned} \quad (11)$$

Since $c_i(d_i)$ and $\frac{\hat{d}_i^2}{2D_i}$ are radially unbounded, the minimization over d and \hat{d} in (10) is always finite for given x and σ . However, whenever $C^T \nu \neq 0$ or $L_a \lambda - CD_a \hat{C}^{bT} \pi - CD_a (\rho^+ - \rho^-) \neq 0$, one can modify P or v to arbitrarily decrease (10). Thus, the infimum is attained if and only if we have

$$C^T \nu = 0 \quad \text{and} \quad (12a)$$

$$L_a \lambda - CD_a \hat{C}^{bT} \pi - CD_a (\rho^+ - \rho^-) = 0. \quad (12b)$$

Moreover, the minimum value must satisfy

$$c_i'(d_i) = \nu_i + \lambda_i \quad \text{and} \quad \frac{\hat{d}_i}{D_i} = \nu_i, \quad \forall i \in \mathcal{N}. \quad (13)$$

Using (12) and (13) we can compute the dual function

$$D(\sigma) = \begin{cases} \Phi(\sigma) & \sigma \in \tilde{\mathcal{N}} \\ -\infty & \text{otherwise,} \end{cases} \quad (14)$$

where

$$\tilde{N} := \left\{ \sigma \in \mathbb{R}^{2|\mathcal{N}|+|\mathcal{K}|+2|\mathcal{E}|} : (12a) \text{ and } (12b) \right\}.$$

and the function $\Phi(\sigma)$ is decoupled in $\sigma_i = (\nu_i, \lambda_i)$, $\sigma_k = (\pi_k)$ and $\sigma_{ij} = (\rho_{ij}^+, \rho_{ij}^-)$. That is,

$$\Phi(\sigma) = \sum_{i \in \mathcal{N}} \Phi_i(\sigma_i) + \sum_{k \in \mathcal{K}} \Phi_k(\sigma_k) + \sum_{ij \in \mathcal{E}} \Phi_{ij}(\sigma_{ij}) \quad (15)$$

where $\Phi_k(\sigma_k) = -\pi_k \hat{P}_k$, $\Phi_{ij}(\sigma_{ij}) = \rho_{ij}^- \underline{P}_{ij} - \rho_{ij}^+ \bar{P}_{ij}$ and

$$\Phi_i(\sigma_i) = c_i(d_i(\sigma_i)) + (\nu_i + \lambda_i)(P_i^m - d_i(\sigma_i)) - \frac{D_i}{2} \nu_i^2, \quad (16)$$

with

$$d_i(\sigma_i) = c_i'^{-1}(\nu_i + \lambda_i). \quad (17)$$

The dual problem of the OLFC (DOLFC) is then given by

DOLFC:

$$\begin{aligned} & \underset{\nu, \lambda, \pi, \rho}{\text{maximize}} && \sum_{i \in \mathcal{N}} \Phi_i(\nu_i, \lambda_i) + \sum_{k \in \mathcal{K}} \Phi_k(\pi_k) + \sum_{ij \in \mathcal{E}} \Phi_{ij}(\rho_{ij}) \\ & \text{subject to} && (12a) \text{ and } (12b) \\ & && \rho_{ij}^+ \geq 0, \quad \rho_{ij}^- \geq 0, \quad ij \in \mathcal{E} \end{aligned} \quad (18)$$

Although $D(\sigma)$ is only finite on \tilde{N} , $\Phi_i(\sigma_i)$, $\Phi_k(\sigma_k)$ and $\Phi_{ij}(\sigma_{ij})$ are finite everywhere. Thus sometimes we use the extended version of the dual function (15) instead of $D(\sigma)$, knowing that $D(\sigma) = \Phi(\sigma)$ for $\sigma \in \tilde{N}$. Given any $S \subset \mathcal{N}$, $K \subset \mathcal{K}$ or $U \subset \mathcal{E}$ we also define $\Phi_S(\sigma_S) := \sum_{i \in S} \Phi_i(\sigma_i)$, $\Phi_K(\sigma_K) := \sum_{k \in K} \Phi_k(\sigma_k)$ and $\Phi_U(\sigma_U) = \sum_{ij \in U} \Phi_{ij}(\sigma_{ij})$ such that $\Phi(\sigma) = \Phi_{\mathcal{N}}(\sigma_{\mathcal{N}}) + \Phi_{\mathcal{K}}(\sigma_{\mathcal{K}}) + \Phi_{\mathcal{E}}(\sigma_{\mathcal{E}})$.

The following lemmas describe several properties of our optimization problem that we will use in latter sections.

Lemma 3 (Strict concavity of $\Phi_S(\sigma_S)$): For any nonempty set $S \subseteq \mathcal{N}$, the function $\Phi_S(\sigma_S)$ is the sum of strictly concave functions $\Phi_i(\sigma_i)$ and it is therefore strictly concave. Moreover, the (extended) dual function $\Phi(\sigma)$ is strictly concave with respect to $\sigma_{\mathcal{N}} = (\nu, \lambda)$.

Proof: From the derivation of $\Phi_i(\sigma_i)$ it is easy to show that

$$\Phi_i(\sigma_i) = \min_{d_i, \hat{d}_i} L_i(d_i, \hat{d}_i, \sigma_i) \quad (19)$$

where

$$L_i(d_i, \hat{d}_i, \sigma_i) := c_i(d_i) + \frac{\hat{d}_i^2}{2D_i} + (\nu_i + \lambda_i)(P_i^m - d_i) - \nu_i \hat{d}_i.$$

Notice that $L_i(d_i, \hat{d}_i, \sigma_i)$ is linear in σ_i and strictly convex in (d_i, \hat{d}_i) .

Let $d_i(\sigma_i)$ and $\hat{d}_i(\sigma_i)$ be the unique minimizer of (19). Then from (13) it follows that $d_i(\sigma_i) = d_i(\nu_i + \lambda_i) = c_i'^{-1}(\nu_i + \lambda_i)$ and $\hat{d}_i(\sigma_i) = D_i \nu_i$.

We will first show that, given $\sigma_{i,1} \neq \sigma_{i,2}$, then

$$(d_i(\sigma_{i,1}), \hat{d}_i(\sigma_{i,1})) \neq (d_i(\sigma_{i,2}), \hat{d}_i(\sigma_{i,2})). \quad (20)$$

Suppose by contradiction that there is $\sigma_{i,1} \neq \sigma_{i,2}$ such that

$$(d_i(\sigma_{i,1}), \hat{d}_i(\sigma_{i,1})) = (d_i(\sigma_{i,2}), \hat{d}_i(\sigma_{i,2})).$$

Then by (13), $c_i'^{-1}(\nu_{i,1} + \lambda_{i,1}) = c_i'^{-1}(\nu_{i,2} + \lambda_{i,2})$ and $D_i \nu_{i,1} = D_i \nu_{i,2}$. Thus, $\nu_{i,1} = \nu_{i,2} = \nu$ and $c_i'^{-1}(\nu + \lambda_{i,1}) = c_i'^{-1}(\nu + \lambda_{i,2})$. But since $c_i(\cdot)$ is strictly convex, c_i' and its inverse are strictly increasing which implies that $\lambda_{i,1} = \lambda_{i,2} = \lambda$. Contradiction.

Finally, let $\theta \in [0, 1]$ and consider any two $\sigma_{i,1} \neq \sigma_{i,2}$. Then,

$$\begin{aligned} \Phi_i(\theta \sigma_{i,1} + (1-\theta)\sigma_{i,2}) &= \min_{d_i, \hat{d}_i} L_i(d_i, \hat{d}_i, \theta \sigma_{i,1} + (1-\theta)\sigma_{i,2}) \\ &= \min_{d_i, \hat{d}_i} \theta L_i(d_i, \hat{d}_i, \sigma_{i,1}) + (1-\theta)L_i(d_i, \hat{d}_i, \sigma_{i,2}) \\ &> \theta \min_{d_i, \hat{d}_i} L_i(d_i, \hat{d}_i, \sigma_{i,1}) + (1-\theta) \min_{d_i, \hat{d}_i} L_i(d_i, \hat{d}_i, \sigma_{i,2}) \\ &= \theta \Phi_i(\sigma_{i,1}) + (1-\theta)\Phi_i(\sigma_{i,2}) \end{aligned}$$

where the strict inequality follows from (20). Thus, $\Phi_i(\sigma_i)$ is strictly concave and by using the definition of strict concavity we get $\Phi_S(\sigma)$ is strictly concave $\forall S \subseteq \mathcal{N}$. ■

Lemma 4 (OLFC Optimality): Given a connected graph $G(\mathcal{N}, \mathcal{E})$, then there exists a scalar ν^* such that $(d^*, \hat{d}^*, x^*, \sigma^*)$ is a primal-dual optimal solution of OLFC and DOLFC if and only if (d^*, \hat{d}^*, x^*) is primal feasible (satisfies (9b)-(9e)), σ^* is dual feasible (satisfies (12) and (18)),

$$\hat{d}_i^* = D_i \nu_i^*, \quad d_i^* = c_i'^{-1}(\nu_i^* + \lambda_i^*), \quad \nu_i^* = \nu^*, \quad i \in \mathcal{N}, \quad (21)$$

and

$$\rho_{ij}^{+*}(a_{ij}(v_i^* - v_j^*) - \bar{P}_{ij}) = 0, \quad ij \in \mathcal{E}, \quad (22a)$$

$$\rho_{ij}^{-*}(\underline{P}_{ij} - a_{ij}(v_i^* - v_j^*)) = 0, \quad ij \in \mathcal{E} \quad (22b)$$

Moreover, d^* , \hat{d}^* , ν^* and λ_i^* are unique with $\nu^* = 0$.

Proof: Assumptions 1 and 2 guarantee that the solution to the primal (OLFC) is finite. Moreover, since by Assumption 2 there is a feasible $d \in \mathcal{D} = \prod_{i=1}^{|\mathcal{N}|} \mathcal{D}_i$, then the Slater condition is satisfied [29] and there is zero duality gap.

Thus, since OLFC only has linear equality constraints, we can use Karush-Kuhn-Tucker (KKT) conditions [29] to characterize the primal dual optimal solution. Thus $(d^*, \hat{d}^*, x^*, \sigma^*)$ is primal dual optimal if and only if we have:

- (i) Primal feasibility: (9b)-(9e)
- (ii) Dual feasibility: (12) and (18)
- (iii) Stationarity:

$$\frac{\partial}{\partial d} L(d, \hat{d}, x, \sigma) = 0, \quad \frac{\partial}{\partial \hat{d}} L(d, \hat{d}, x, \sigma) = 0$$

$$\text{and} \quad \frac{\partial}{\partial x} L(d, \hat{d}, x, \sigma) = 0.$$

- (iv) Complementary slackness:

$$\rho_{ij}^{+*}(a_{ij}(v_i^* - v_j^*) - \bar{P}_{ij}) = 0, \quad ij \in \mathcal{E}$$

and

$$\rho_{ij}^{-*}(\underline{P}_{ij} - a_{ij}(v_i^* - v_j^*)) = 0, \quad ij \in \mathcal{E}.$$

KKT conditions (i), (ii) and (iv) are already implicit by assumptions of the lemma. Furthermore, since the graph G is connected then (12a) is equivalent to

$$\nu_i^* = \nu^* \quad \forall i \in \mathcal{N}.$$

which is the third condition of (21).

Now, using (11), Stationarity (iii) is equivalent to (ii) and

$$\frac{\partial L}{\partial d_i}(d^*, \hat{d}^*, x^*, \sigma^*) = c'_i(d_i^*) - (\nu_i^* + \lambda_i^*) = 0 \quad (23a)$$

$$\frac{\partial L}{\partial \hat{d}_i}L(d^*, \hat{d}^*, x^*, \sigma^*) = \frac{\hat{d}_i^*}{D_i} - \nu_i^* = 0 \quad (23b)$$

which are the remaining conditions of (21).

Since $c_i(d_i)$ and $\frac{\hat{d}_i^2}{2D_i}$ are strictly convex functions, by the same argument in the proof of Lemma 3 we get that ν_i^* and λ_i^* are unique. To show $\nu^* = 0$ we use (i). Adding (9b) over $i \in \mathcal{N}$ gives

$$\begin{aligned} 0 &= \sum_{i \in \mathcal{N}} \left(P_i^m - (d_i^* + \hat{d}_i^*) - \sum_{e \in \mathcal{E}} C_{ie} P_e \right) \\ &= \sum_{i \in \mathcal{N}} \left(P_i^m - (d_i^* + \hat{d}_i^*) \right) - \sum_{e=ij \in \mathcal{E}} (C_{ie} P_e + C_{je} P_e) \\ &= \sum_{i \in \mathcal{N}} \left(P_i^m - (d_i^* + \hat{d}_i^*) \right) \end{aligned} \quad (24)$$

and similarly (9c) gives

$$0 = \sum_{i \in \mathcal{N}} P_i^m - d_i^* \quad (25)$$

Thus, subtracting (24) from (25) gives $0 = \sum_{i \in \mathcal{N}} \hat{d}_i^* = \sum_{i \in \mathcal{N}} D_i \nu_i^* = \nu^* \sum_{i \in \mathcal{N}} D_i$ and since $D_i > 0 \forall i \in \mathcal{N}$, it follows that $\nu^* = 0$. ■

IV. DISTRIBUTED OPTIMAL LOAD CONTROL

We show how we can leverage the power network dynamics to solve the OLFC problem in a distributed way. Our solution is based on the classical primal dual optimization algorithm that has been of great use to design congestion control mechanisms in communication networks [30]–[33].

Let

$$\begin{aligned} L(x, \sigma) &= \underset{d, \hat{d}}{\text{minimize}} \quad L(d, \hat{d}, x, \sigma) \\ &= L(d(\sigma), \hat{d}(\sigma), x, \sigma) \\ &= \Phi(\sigma) - P^T C^T \nu \\ &\quad - v^T (L_a \lambda - C D_a \hat{C}^b T \pi - C D_a (\rho^+ - \rho^-)) \end{aligned} \quad (26)$$

where $L(d, \hat{d}, x, \sigma)$ is defined as in (11), $d(\sigma) := (d_i(\sigma_i))$ and $\hat{d}(\sigma) := (\hat{d}_i(\sigma_i))$ according to (21).

Similarly to [28] we propose the following partial primal-dual law

$$\dot{\nu}_{\mathcal{G}} = \zeta_{\mathcal{G}}^{\nu} (P_{\mathcal{G}}^m - (d_{\mathcal{G}}(\sigma_{\mathcal{G}}) + D_{\mathcal{G}} \nu_{\mathcal{G}}) - C_{\mathcal{G}} P) \quad (27a)$$

$$0 = P_{\mathcal{L}}^m - (d_{\mathcal{L}}(\sigma_{\mathcal{L}}) + D_{\mathcal{L}} \nu_{\mathcal{L}}) - C_{\mathcal{L}} P \quad (27b)$$

$$\dot{\lambda} = \zeta^{\lambda} (P^m - d(\sigma) - L_a v) \quad (27c)$$

$$\dot{\pi} = \zeta^{\pi} (\hat{C}^b D_a C^T v - \hat{P}) \quad (27d)$$

$$\dot{\rho}^+ = \zeta^{\rho^+} [D_a C^T v - \bar{P}]_{\rho^+}^+ \quad (27e)$$

$$\dot{\rho}^- = \zeta^{\rho^-} [P - D_a C^T v]_{\rho^-}^+ \quad (27f)$$

$$\dot{P} = \chi^P (C^T \nu) \quad (27g)$$

$$\dot{v} = \chi^v (L_a \lambda - C D_a \hat{C}^b T \pi - C D_a (\rho^+ - \rho^-)) \quad (27h)$$

where $\zeta_{\mathcal{G}}^{\nu} = \text{diag}(\zeta_i^{\nu})_{i \in \mathcal{G}}$, $\zeta^{\lambda} = \text{diag}(\zeta_i^{\lambda})_{i \in \mathcal{N}}$, $\zeta^{\pi} = \text{diag}(\zeta_k^{\pi})_{k \in \mathcal{K}}$, $\zeta^{\rho^+} = \text{diag}(\zeta_e^{\rho^+})_{e \in \mathcal{E}}$, $\zeta^{\rho^-} = \text{diag}(\zeta_e^{\rho^-})_{e \in \mathcal{E}}$, $\chi^P = \text{diag}(\chi_e^P)_{e \in \mathcal{E}}$ and $\chi^v = \text{diag}(\chi_i^v)_{i \in \mathcal{N}}$.

The operator $[\cdot]_u^+$ is an element-wise projection that maintains each element of the $u(t)$ within the positive orthant when $\dot{u} = [\cdot]_u^+$, i.e. given any vector a with same dimension as u then $[a]_u^+$ is defined element-wise by

$$[a_e]_{u_e}^+ = \begin{cases} a_e & \text{if } a_e > 0 \text{ or } u_e > 0, \\ 0 & \text{otherwise.} \end{cases} \quad (28)$$

One property that will be used later is that given any constant vector $u^* \geq 0$, then

$$(u - u^*)^T [a]_u^+ \leq (u - u^*)^T a \quad (29)$$

since for any pair (u_e, a_e) that makes the projection active we must have by definition $u_e = 0$ and $a_e < 0$ and therefore

$$(u_e - u_e^*) a_e = -u_e^* a_e \geq 0 = (u_e - u_e^*)^T [a_e]_{u_e}^+.$$

Equations (27a), (27b) and (27g) show that dynamics (1) can be interpreted as a subset of the primal-dual dynamics described in (27) for the special case when $\zeta_i^{\nu} = M_i^{-1}$ and $\chi_{ij}^P = B_{ij}$. Therefore, we can interpret the frequency ω_i as the Lagrange multiplier ν_i .

This observation motivates us to propose a distributed load control scheme that is naturally decomposed into

Power Network Dynamics:

$$\dot{\omega}_{\mathcal{G}} = M_{\mathcal{G}}^{-1} (P_{\mathcal{G}}^m - (d_{\mathcal{G}} + \hat{d}_{\mathcal{G}}) - C_{\mathcal{G}} P) \quad (30a)$$

$$0 = P_{\mathcal{L}}^m - (d_{\mathcal{L}} + \hat{d}_{\mathcal{L}}) - C_{\mathcal{L}} P \quad (30b)$$

$$\dot{P} = D_B C^T \omega \quad (30c)$$

$$\hat{d} = D \omega \quad (30d)$$

and

Dynamic Load Control:

$$\dot{\lambda} = \zeta^{\lambda} (P^m - d(\sigma) - L_a v) \quad (31a)$$

$$\dot{\pi} = \zeta^{\pi} (\hat{C}^b D_a C^T v - \hat{P}) \quad (31b)$$

$$\dot{\rho}^+ = \zeta^{\rho^+} [D_a C^T v - \bar{P}]_{\rho^+}^+ \quad (31c)$$

$$\dot{\rho}^- = \zeta^{\rho^-} [P - D_a C^T v]_{\rho^-}^+ \quad (31d)$$

$$\dot{v} = \chi^v (L_a \lambda - C D_a \hat{C}^b T \pi - C D_a (\rho^+ - \rho^-)) \quad (31e)$$

$$d = c'^{-1} (\omega + \lambda) \quad (31f)$$

Equations (30) and (31) show how the network dynamics can be complemented with dynamic load control such that the whole system amounts to a distributed primal-dual algorithm that tries to find a saddle point on $L(x, \sigma)$. The next section shows that this system does achieve optimality as intended.

V. OPTIMALITY AND CONVERGENCE ANALYSIS

In this section we will show that the system (30)–(31) can fairly rebalance supply and demand, restore the nominal frequency, and preserve inter-area flow schedules and thermal limits.

We will achieve this objective in two steps. Firstly, we will show that every equilibrium point of (30)-(31) is an optimal solution of (9). This guarantees that a stationary point of the system balances supply and demand, is fair among the controllable loads, and achieves zero frequency deviation.

Secondly, we will show that every trajectory $(d(t), \hat{d}_i(t), P(t), v(t), \omega(t), \lambda(t), \pi(t), \rho^+(t), \rho^-(t))$ converges to an equilibrium point of (30)-(31). Moreover, the equilibrium point will satisfy (2) and (5) under mild conditions.

Theorem 5 (Optimality): Given a point $p^* = (d^*, \hat{d}^*, x^*, \sigma^*)$, then p^* is an equilibrium point of (30)-(31) if and only if it is a primal-dual optimal solution to the OLFC problem.

Proof: The proof of this theorem is a direct application of Lemma 4. Let $(d^*, \hat{d}^*, x^*, \sigma^*)$ be an equilibrium point of (30)-(31). Then, by (30c) and (31c)-(31e), σ^* is dual feasible.

Similarly, since $\dot{\omega}_i = 0$, $\dot{\lambda}_i = 0$, $\dot{\pi}_k = 0$, $\dot{\rho}_{ij}^+ = 0$ and $\dot{\rho}_{ij}^- = 0$, then (30a)-(30b) and (31a)-(31d) are equivalent to primal feasibility, i.e. $(d^*, \hat{d}^*, P^*, v^*)$ is a feasible point of (9). Finally, by definition of (30)-(31) conditions (21) and (22) are always satisfied by any equilibrium point. Thus we are under the conditions of Lemma 4 and therefore $p^* = (d^*, \hat{d}^*, x^*, \sigma^*)$ is primal-dual optimal which also implies that $\omega^* = 0$. ■

Remark 6: Theorem 5 implies that every equilibrium solution of (30)-(31) is optimal with respect to OLFC. However, it guarantees neither convergence to it nor that the line flows satisfy (2) and (5).

The rest of this section is devoted to showing that in fact for every initial condition $(P(0), v(0), \omega(0), \lambda(0), \pi(0), \rho^+(0), \rho^-(0))$, the system (30)-(31) converges to one of such optimal solution. Furthermore, we will show that, under mild assumption on D_a and $P(0)$, $P(t)$ converges to a P^* that satisfies (2) and (5).

Since we showed in Section IV that (30)-(31) are just a special case of (27), we will provide our convergence result for (27). Our global convergence proof leverages the results of [34] on global convergence in network flow control. Unfortunately, the results presented there cannot be readily applied as (27) is not a full primal-dual gradient law due to constraint (27b). However, the next lemma shows that (27) amounts to a primal-dual gradient law with respect to a different Lagrangian.

Lemma 7 (Primal-dual Gradient Law): Let $y = (\nu_{\mathcal{L}}, \lambda, \pi, \rho)^1$ and consider the reduced Lagrangian

$$L(x, y) = \underset{\nu_{\mathcal{L}}}{\text{maximize}} L(x, \sigma). \quad (32)$$

Then, $L(x, y)$ is concave in y , convex in x and the dynamics (27) amount to

$$\dot{y} = Y \left[\frac{\partial}{\partial y} L(x, y)^T \right]_{\rho}^+ \quad \text{and} \quad \dot{x} = -X \frac{\partial}{\partial x} L(x, y)^T \quad (33)$$

where the projection $[a]_{\rho}^+$ only acts in the ρ positions of a , $Y = \text{blockdiag}(\zeta_{\mathcal{G}}^{\nu}, \zeta^{\lambda}, \zeta^{\pi}, \zeta^{\rho^+}, \zeta^{\rho^-})$ and $X = \text{blockdiag}(\chi^P, \chi^v)$.

¹Recall that $\rho = (\rho^+, \rho^-)$

Moreover, under Assumption 1, any saddle point (x^*, y^*) of $L(x, y)$ is unique in $\nu_{\mathcal{L}}$ and λ .

Proof:

By Lemma 3 and (26), $L(x, \sigma)$ is strictly concave in $\sigma_{\mathcal{N}} = (\nu, \lambda)$. Therefore, it follows that there exists a unique

$$\nu_{\mathcal{L}}^*(x, y) = \arg \max_{\nu_{\mathcal{L}}} L(x, \sigma). \quad (34)$$

Moreover, by stationarity, $\nu_{\mathcal{L}}^*(x, y)$ must satisfy

$$\frac{\partial L}{\partial \nu_{\mathcal{L}}}(x, y, \nu_{\mathcal{L}}^*(x, y)) = \quad (35a)$$

$$= \frac{\partial \Phi_{\mathcal{L}}}{\partial \nu_{\mathcal{L}}}(y, \nu_{\mathcal{L}}^*(x, y)) - (C_{\mathcal{L}}P)^T = 0 \quad (35b)$$

which is equivalent to (27b), i.e. $\nu_{\mathcal{L}}^*(x, y)$ implicitly satisfies (27b).

We now apply the envelope theorem [35] on (32) to compute $\frac{\partial}{\partial x} L(x, y)$ and $\frac{\partial}{\partial y} L(x, y)$ using

$$\frac{\partial}{\partial x} L(x, y) = \frac{\partial}{\partial x} L(x, y, \nu_{\mathcal{L}}) \Big|_{\nu_{\mathcal{L}}^*(x, y)} \quad (36a)$$

$$\frac{\partial}{\partial y} L(x, y) = \frac{\partial}{\partial y} L(x, y, \nu_{\mathcal{L}}) \Big|_{\nu_{\mathcal{L}}^*(x, y)} \quad (36b)$$

Using equation (36), (33) only differs from (27a) and (27c)-(27h) on the locations where $\nu_{\mathcal{L}}$ must be substituted with $\nu_{\mathcal{L}}^*(x, y)$. However, since there is a unique $\nu_{\mathcal{L}}$ that satisfies (27b), then it follows that (33) and (27) are equivalent representations of the same system.

Finally, given any saddle-point of (x^*, y^*) , $(d^*, \hat{d}^*, x^*, y^*, \nu_{\mathcal{L}}^*)$ is a saddle point of $L(d, \hat{d}, x, \sigma)$. Therefore, using Lemma 4 the uniqueness properties follow. ■

We will also use the following results in our convergence proof.

Lemma 8 (Differentiability of $\nu_{\mathcal{L}}^(x, y)$):* Given any (x, y) , the maximizer of (32), $\nu_{\mathcal{L}}^*(x, y)$, is continuously differentiable provided $c_i(\cdot)$ is strongly convex. Furthermore, the derivative is given by

$$\frac{\partial}{\partial x} \nu_{\mathcal{L}}^*(x, y) = \left[-(D_{\mathcal{L}} + d'_{\mathcal{L}})^{-1} C_{\mathcal{L}} \mid 0 \right]_{\nu_{\mathcal{L}}} \quad (37)$$

$$\frac{\partial}{\partial y} \nu_{\mathcal{L}}^*(x, y) = \left[0 \mid 0 \mid -(D_{\mathcal{L}} + d'_{\mathcal{L}})^{-1} \hat{d}'_{\mathcal{L}} \mid 0 \mid 0 \right]_{\nu_{\mathcal{L}}} \quad (38)$$

where $D_S := \text{diag}(D_i)_{i \in S}$ and

$$d'_S = \begin{cases} \text{diag}(d'_i(\lambda_i + \nu_i^*(x, y)))_{i \in S} & \text{if } S \subseteq \mathcal{L} \\ \text{diag}(d'_i(\lambda_i + \nu_i))_{i \in S} & \text{if } S \subseteq \mathcal{G} \end{cases}$$

Proof: We first notice that $\nu_i^*(x, y)$, $i \in \mathcal{L}$, depends only on λ_i and $C_i P := \sum_{e \in E} C_{i,e} P_e$. Which means that $\frac{\partial}{\partial v} \nu_{\mathcal{L}}^*(x, y) = 0$, $\frac{\partial}{\partial \nu_{\mathcal{G}}} \nu_{\mathcal{L}}^*(x, y) = 0$, $\frac{\partial}{\partial \pi} \nu_{\mathcal{L}}^*(x, y) = 0$, $\frac{\partial}{\partial \rho} \nu_{\mathcal{L}}^*(x, y) = 0$ and $\frac{\partial}{\partial \lambda_{\mathcal{L}}} \nu_{\mathcal{L}}^*(x, y)$ is diagonal.

Now, by definition of $\nu_{\mathcal{L}}^*(x, y)$, for any $i \in \mathcal{L}$ we have

$$\frac{\partial}{\partial \nu_i} L(x, y, \nu_{\mathcal{L}}^*(x, y)) = \quad (39)$$

$$= P_i^m - (D_i \nu_i^*(x, y) + d_i(\lambda_i + \nu_i^*(x, y))) - \sum_{e \in E} C_{i,e} P_e \quad (40)$$

$$= 0 \quad (41)$$

Therefore, if we fix P and take the total derivative of $\frac{\partial}{\partial \nu_i} L(x, y, \nu_{\mathcal{L}}^*(x, y))$ with respect to λ_i we obtain

$$0 = \frac{d}{d\lambda_i} \left(\frac{\partial}{\partial \nu_i} L(x, y, \nu_{\mathcal{L}}^*(x, y)) \right) \quad (42)$$

$$= -(D_i + d'_i(\lambda_i + \nu_i^*)) \frac{\partial}{\partial \lambda_i} \nu_i^* - d'_i(\lambda_i + \nu_i^*) \quad (43)$$

where here we used ν_i^* for short of $\nu_i^*(x, y)$.

Now since by assumption $c_i(\cdot)$ is strongly convex, i.e. $c_i''(\cdot) \geq \alpha$, $d'_i(\cdot) = \frac{1}{c_i'(\cdot)} \leq \frac{1}{\alpha} < \infty$. Thus, $(D_i + d'_i)$ is finite and strictly positive, which implies that

$$\frac{\partial}{\partial \lambda_i} \nu_i^*(x, y) = -\frac{d'_i(\lambda_i + \nu_i^*(x, y))}{(D_i + d'_i(\lambda_i + \nu_i^*(x, y)))}, \quad i \in \mathcal{L}.$$

Similarly, we obtain

$$\frac{\partial}{\partial P} \nu_i^*(x, y) = -\frac{1}{(D_i + d'_i(\lambda_i + \nu_i^*(x, y)))} C_i, \quad i \in \mathcal{L}.$$

where C_i is the i th row of C .

Notice that whenever $d'_i(\lambda_i + \nu_i^*)$ exists, then $\frac{\partial}{\partial x} \nu_i^*$ and $\frac{\partial}{\partial y} \nu_i^*$ also exists. ■

Lemma 9 (Second order derivatives of $L(x, y)$):

Whenever Lemma 8 holds, then we have

$$\frac{\partial^2}{\partial x^2} L(x, y) = \begin{bmatrix} C_{\mathcal{L}}^T (D_{\mathcal{L}} + d'_{\mathcal{L}})^{-1} C_{\mathcal{L}} & 0 \\ 0 & 0 \end{bmatrix} \begin{matrix} P \\ v \end{matrix} \quad (44)$$

and

$$\frac{\partial^2}{\partial y^2} L(x, y) = - \begin{bmatrix} \nu_{\mathcal{G}} & \lambda_{\mathcal{G}} & \lambda_{\mathcal{L}} & \pi & \rho \\ (D_{\mathcal{G}} + d'_{\mathcal{G}}) & d'_{\mathcal{G}} & 0 & 0 & 0 \\ d'_{\mathcal{G}} & d'_{\mathcal{G}} & 0 & 0 & 0 \\ 0 & 0 & D_{\mathcal{L}}(D_{\mathcal{L}} + d'_{\mathcal{L}})^{-1} d'_{\mathcal{L}} & 0 & 0 \\ 0 & 0 & 0 & 0 & 0 \\ 0 & 0 & 0 & 0 & 0 \end{bmatrix} \begin{matrix} \nu_{\mathcal{G}} \\ \lambda_{\mathcal{G}} \\ \lambda_{\mathcal{L}} \\ \pi \\ \rho \end{matrix} \quad (45)$$

with $\frac{\partial^2}{\partial x^2} L(x, y) \succeq 0$ and $\frac{\partial^2}{\partial y^2} L(x, y) \preceq 0$.

Proof: Using envelope theorem [35] in (32) we have

$$\frac{\partial L}{\partial x}(x, y) = \frac{\partial L}{\partial x}(x, y, \nu_{\mathcal{L}}^*(x, y))$$

which implies that

$$\begin{aligned} \frac{\partial^2 L}{\partial x^2}(x, y) &= \frac{\partial}{\partial x} \left[\frac{\partial L}{\partial x}(x, y, \nu_{\mathcal{L}}^*(x, y)) \right] \\ &= \frac{\partial^2 L}{\partial x^2}(x, y, \nu_{\mathcal{L}}^*(x, y)) + \frac{\partial^2 L}{\partial x \partial \nu_{\mathcal{L}}}(x, y, \nu_{\mathcal{L}}^*(x, y)) \frac{\partial}{\partial x} \nu_{\mathcal{L}}^*(x, y) \\ &= \frac{\partial^2 L}{\partial x \partial \nu_{\mathcal{L}}}(x, y, \nu_{\mathcal{L}}^*(x, y)) \frac{\partial}{\partial x} \nu_{\mathcal{L}}^*(x, y). \end{aligned} \quad (46)$$

where the last step follow from $L(x, \sigma)$ being linear in x .

Now, by definition of $\nu_{\mathcal{L}}^*(x, y)$ it follows that

$$\frac{\partial L}{\partial \nu_{\mathcal{L}}}(x, y, \nu_{\mathcal{L}}^*(x, y)) = 0. \quad (47)$$

Differentiating (47) with respect to x gives

$$0 = \frac{\partial^2 L}{\partial \nu_{\mathcal{L}} \partial x}(x, y, \nu_{\mathcal{L}}^*(x, y)) + \frac{\partial^2 L}{\partial \nu_{\mathcal{L}}^2}(x, y, \nu_{\mathcal{L}}^*(x, y)) \frac{\partial}{\partial x} \nu_{\mathcal{L}}^*(x, y)$$

and therefore

$$\begin{aligned} \frac{\partial^2 L}{\partial x \partial \nu_{\mathcal{L}}}(x, y, \nu_{\mathcal{L}}^*(x, y)) &= \left[\frac{\partial^2 L}{\partial \nu_{\mathcal{L}} \partial x}(x, y, \nu_{\mathcal{L}}^*(x, y)) \right]^T \\ &= -\frac{\partial}{\partial x} \nu_{\mathcal{L}}^*(x, y)^T \frac{\partial^2 L}{\partial \nu_{\mathcal{L}}^2}(x, y, \nu_{\mathcal{L}}^*(x, y)). \end{aligned} \quad (48)$$

Substituting (48) into (46) gives

$$\frac{\partial^2 L}{\partial x^2}(x, y) = -\frac{\partial}{\partial x} \nu_{\mathcal{L}}^*(x, y)^T \frac{\partial^2 L}{\partial \nu_{\mathcal{L}}^2}(x, y, \nu_{\mathcal{L}}^*(x, y)) \frac{\partial}{\partial x} \nu_{\mathcal{L}}^*(x, y). \quad (49)$$

It follows from (35) and (16) that

$$\begin{aligned} \frac{\partial^2 L}{\partial \nu_{\mathcal{L}}^2}(x, y, \nu_{\mathcal{L}}^*(x, y)) &= \frac{\partial^2 \Phi_{\mathcal{L}}}{\partial \nu_{\mathcal{L}}^2}(\nu_{\mathcal{L}}^*(x, y), \lambda_{\mathcal{L}}) \\ &= -(D_{\mathcal{L}} + d'_{\mathcal{L}}). \end{aligned} \quad (50)$$

Therefore, substituting (37) and (50) into (49) gives (44).

A similar calculation using (38) gives (45). ■

We now present our main convergence result. Let E be the set of equilibrium points of (27)

$$E := \left\{ (x, \sigma) : \frac{\partial L}{\partial x}(x, \sigma) = 0, \frac{\partial L}{\partial \sigma}(x, \sigma) = 0 \right\},$$

which by Theorem 5 is the set of optimal solutions of the OLFC problem.

Theorem 10 (Global Convergence): The set E of equilibrium points of the partial primal dual algorithm (27) is globally asymptotically stable. Furthermore, each individual trajectory converges to a unique point within E that is optimal with respect to the OLFC problem.

Proof: By Lemma 7, we know that partial primal-dual dynamics (27) can be interpreted as a complete primal-dual gradient law of the reduced Lagrangian (32). Therefore, following [34] we consider the candidate Lyapunov function

$$U(z) = (z - z^*)^T Z^{-1} (z - z^*) \quad (51)$$

where $z = (x, y)$, $Z = \text{blockdiag}(X, Y)$ and $z^* = (x^*, y^*)$ is any equilibrium point of (33).

Let $f(z) = [-\frac{\partial}{\partial x} L(x, y) \quad \frac{\partial}{\partial y} L(x, y)]^T$ such that (33) becomes

$$\dot{z} = Z[f(z)]_+^+. \quad (52)$$

Notice that $f(z^*) = 0$ for all optimal solutions $z^* = (x^*, y^*)$.

Then it follows from Lemma 7 that

$$\dot{U}(z) = \frac{1}{2}((z - z^*)^T [f(z)]_\rho^+ + [f(z)]_\rho^+ (z - z^*)) \quad (53)$$

$$\leq \frac{1}{2}((z - z^*)^T f(z) + f(z)^T (z - z^*)) \quad (54)$$

$$= \frac{1}{2} \int_0^1 (z - z^*)^T \left[\frac{\partial}{\partial z} f(z(s))^T + \frac{\partial}{\partial z} f(z(s)) \right] (z - z^*) ds \quad (55)$$

$$= \underbrace{\int_0^1 (x - x^*)^T \left[-\frac{\partial^2}{\partial x^2} L(x(s), y(s)) \right] (x - x^*) ds}_{\leq 0} \quad (56)$$

$$+ \underbrace{\int_0^1 (y - y^*)^T \left[\frac{\partial^2}{\partial y^2} L(x(s), y(s)) \right] (y - y^*) ds}_{\leq 0} \quad (57)$$

where (53) follows from (52) and (54) from (29). The vector $z(s) = (x(s), y(s)) := (z - z^*)s + z^*$, and (55) follows from the fact that $f(z) = f(z) - f(z^*) = \int_0^1 \frac{\partial}{\partial z} f(z(s))(z - z^*) ds$. Finally, equations (56) and (57) follow from the definition of $f(z)$ and z .

Therefore, since $U(x, y)$ is radially unbounded, Lasalle's Invariance Principle [36] asserts that the trajectories $(x(t), y(t))$ converge to the largest invariance set within $\{\dot{U}(x, y) \equiv 0\}$. This implies that the trajectories $(x(t), \sigma(t))$ of (27) must converge to the largest invariant set

$$M \subseteq \{(x, \sigma) : \nu_{\mathcal{L}} = \nu_{\mathcal{L}}^*(x, y), \dot{U}(x, y) \equiv 0\}.$$

We now characterize M . Notice that in order to have $\dot{U} \equiv 0$, then both terms (56) and (57) must be zero.

Using Lemma 9, it follows that

$$\int_0^1 (x - x^*)^T \left[-\frac{\partial^2}{\partial x^2} L(x(s), y(s)) \right] (x - x^*) ds \equiv 0$$

if and only if

$$(P - P^*)^T C_{\mathcal{L}}^T (D_{\mathcal{L}} + d'_{\mathcal{L}})^{-1} C_{\mathcal{L}} (P - P^*) \equiv 0$$

which implies $C_{\mathcal{L}} P \equiv C_{\mathcal{L}} P^*$ since $(D_{\mathcal{L}} + d'_{\mathcal{L}})^{-1} \succ 0$.

A similar argument for (57) gives

$$\nu_i(t) \equiv 0, \quad i \in \mathcal{G} \text{ and } \lambda_i(t) \equiv \lambda_i^*, \quad i \in \mathcal{N} \quad (58)$$

Therefore, since $C_{\mathcal{L}} P \equiv C_{\mathcal{L}} P^*$, (58) together with (27b) implies that

$$\nu_{\mathcal{L}}^*(x(t), y(t)) \equiv \hat{\nu}_{\mathcal{L}} \quad (59)$$

where $\hat{\nu}_{\mathcal{L}}$ is not necessarily zero.

We have obtained so far: $\nu(t) \equiv \hat{\nu}$ and $\lambda(t) \equiv \lambda^*$.

Now, since $\dot{\lambda} = 0$, it follows from (27c) that $C^T v(t) \equiv C^T \hat{v}$ for some constant vector \hat{v} or equivalently $v(t) \equiv \hat{v} + \beta(t)\mathbf{1}$. Differentiating in time $\mathbf{1}^T (\chi^v)^{-1} v(t)$ gives $0 = \mathbf{1}^T (\chi^v)^{-1} \dot{v} = (\sum_{i \in \mathcal{N}} \frac{1}{\chi_i^v}) \dot{\beta}$ which implies that $\beta(t) \equiv \hat{\beta}$.

Suppose now that either $\dot{P} \neq 0$ or $\dot{\pi} \neq 0$. Since $C^T v(t) \equiv C^T \hat{v}$ and $\nu(t) \equiv \hat{\nu}$, \dot{P} and $\dot{\pi}$ are constant. Thus, since the trajectories are bounded, we must have $\dot{P} = 0$ and $\dot{\pi} = 0$; otherwise $U(x, y)$ will grow unboundedly (contradiction).

It remains to show that $\dot{\rho} = 0$, i.e. $\dot{\rho}^+ = \dot{\rho}^- = 0$. Since $v(t) \equiv \hat{v}$, then argument inside (27e) and (27f) is constant.

Now consider any ρ_e^+ , $e \in \mathcal{E}$. Then we have three cases: (i) $a_e(\hat{v}_i - \hat{v}_j) - \bar{P}_e > 0$, (ii) $a_e(\hat{v}_i - \hat{v}_j) - \bar{P}_e < 0$ and (iii) $a_e(\hat{v}_i - \hat{v}_j) - \bar{P}_e = 0$. Case (i) implies $\rho_e^+(t) \rightarrow \infty$ which cannot happen since the trajectories are bounded. Case (ii) implies that $\rho_e^+(t) \equiv 0$ which implies that $\dot{\rho}_e^+ = 0$, and case (iii) also implies $\dot{\rho}_e^+ = 0$. An analogous argument gives $\dot{\rho}^- = 0$.

Thus, we have shown that $M \subseteq E$. Unfortunately, since there is an affine space of equilibria (x^*, σ^*) in E , Krasovskii-Lassale Invariance Principle does not guarantee that $(x(t), \sigma(t))$ will converge to one specific (x^*, σ^*) value.

Fortunately, we can use structure of $U(x, y)$ as in [23] to achieve convergence to a single equilibrium. Since $(x(t), \sigma(t)) \rightarrow M$ and $(x(t), \sigma(t))$ are bounded, then there exists an infinite sequence of time values $\{t_k\}$ such that $(x(t_k), \sigma(t_k)) \rightarrow (\hat{x}^*, \hat{y}^*, \hat{\nu}_{\mathcal{L}}^*) \in M$. Thus, using this specific equilibrium (\hat{x}^*, \hat{y}^*) in the definition of $U(x, y)$, it follows that $U(x(t_k), y(t_k)) \rightarrow 0$, which by continuity of $U(x, y)$ implies that $(x(t), y(t)) \rightarrow (\hat{x}^*, \hat{y}^*)$.

Thus, it follows that $(x(t), \sigma(t))$ converges to only one optimal solution within $M \subseteq E$. ■

Finally, the following theorem show that under mild conditions the system is able to restore the inter-area flows (2) and maintain the line flows within the thermal limits (5).

Theorem 11 (Inter-area Constraints and Thermal Limits): Given any primal-dual optimal solution $(x^*, \sigma^*) \in E$, the optimal line flow vector P^* satisfies (2). Furthermore, if $P(0) = D_B C^T \theta^0$ and $a_{ij} = B_{ij}$, then $P_{ij}^* = a_{ij}(v_i^* - v_j^*)$ and therefore (5) holds.

Proof: By optimality, P^* and v^* must satisfy

$$P^m - d^* = C P^* = L_a v^* = C D_a C^T v^* \quad (60)$$

Therefore using primal feasibility, (3) and (60) we have

$$\begin{aligned} \hat{P} &= \hat{C}^{\flat} D_a C^T v^* = E_{\mathcal{K}} C D_a C^T v^* \\ &= E_{\mathcal{K}} C P^* = \hat{C}^{\flat} P^* \end{aligned}$$

which is exactly (4).

Finally, to show that $P_{ij}^* = a_{ij}(v_i^* - v_j^*)$ we will use (30c). Integrating (30c) over time gives

$$P(t) - P(0) = \int_0^t D_B C^T \nu(s) ds.$$

Therefore, since $P(t) \rightarrow P^*$, we have $P^* = P(0) + D_B C^T \theta^*$ where θ^* is any finite vector satisfying $C^T \theta^* = \int_0^\infty C^T \nu(s) ds$.

Again by primal feasibility

$$\begin{aligned} C D_a C^T v^* &= L_a v^* = C P^* = C(P(0) + D_B C^T \theta^*) \\ &= C D_B C^T (\theta^0 + \theta^*) \end{aligned}$$

Since by assumption $D_a = D_B$ then we must have $v^* = (\theta^0 + \theta^*) + \alpha \mathbf{1}$ and it follows then that $P^* = D_B C^T (\theta^0 + \theta^*) = D_B C^T (v^* - \alpha \mathbf{1}) = D_a C^T v^*$. Therefore, since by primal feasibility $\underline{P} \leq D_a C^T v^* \leq \bar{P}$, then $\underline{P} \leq P^* \leq \bar{P}$. ■

Remark 12: The assumption of Theorem 11 of having $P(0) = D_B C^T \theta^0$ is equivalent to substituting (30) with

$$\dot{\omega}_G = M_G^{-1} (P_G^m - (d_G + D_G \omega_G) - C_G D_B C^T \theta) \quad (61a)$$

$$0 = P_L^m - (d_L + D_L \omega_L) - C_L D_B C^T \theta \quad (61b)$$

$$\dot{\theta} = \omega \quad (61c)$$

which is the linearization of the power network using phase instead of line flows as states. Therefore, this assumption can be done without loss of generality.

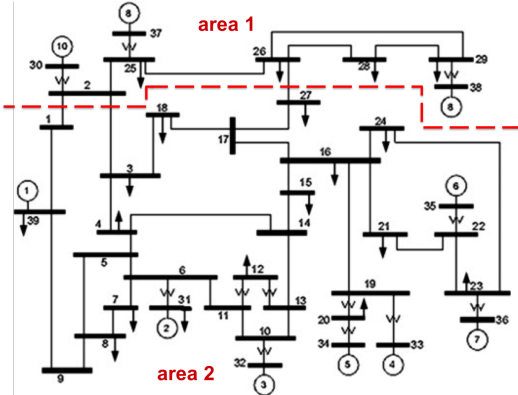


Fig. 1: IEEE 39 bus system: New England

VI. NUMERICAL ILLUSTRATIONS

We now illustrate the behavior of our control scheme. We consider the widely used IEEE 39 bus system, shown in Figure 1, to test our scheme. We assume that the system has two independent control areas that are connected through lines (1, 2), (2, 3) and (26, 27). The network parameters as well as the initial stationary point (pre fault state) were obtained from the Power System Toolbox [37] data set.

Each bus is assumed to have a controllable load with $\mathcal{D}_i = [-d_{\max}, d_{\max}]$, with $d_{\max} = 1$ p.u. on a 100MVA base and disutility function

$$\begin{aligned} c_i(d_i) &= \int_0^{d_i} \tan\left(\frac{\pi}{2d_{\max}} s\right) ds \\ &= -\frac{2d_{\max}}{\pi} \ln\left(\left|\cos\left(\frac{\pi}{2d_{\max}} d_i\right)\right|\right). \end{aligned}$$

Thus, $d_i(\sigma_i) = c_i'^{-1}(\omega_i + \lambda_i) = \frac{2d_{\max}}{\pi} \arctan(\omega_i + \lambda_i)$. See Figure 2 for an illustration of both $c_i(d_i)$ and $d_i(\sigma_i)$.

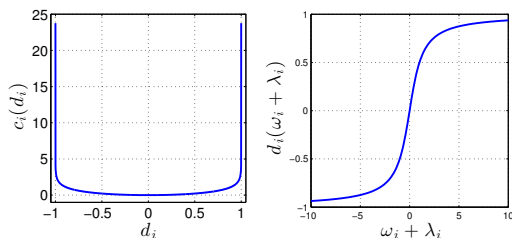


Fig. 2: Disutility $c_i(d_i)$ and load function $d_i(\omega_i + \lambda_i)$

Throughout the simulations we assume that the aggregate generator damping and load frequency sensitivity parameter

$D_i = 0.2 \forall i \in \mathcal{N}$ and $\chi_i^v = \zeta_i^\lambda = \zeta_k^\pi = \zeta_e^{\rho^+} = \zeta_e^{\rho^-} = 2$, for all $i \in \mathcal{N}$, $k \in \mathcal{K}$ and $e \in \mathcal{E}$. These parameter values do not affect convergence, but in general they will affect the convergence rate. The values of P^m are corrected so that they initially add up to zero by evenly distributing the mismatch among the load buses. \hat{P} is obtained from the starting stationary condition. We initially set \bar{P} and \underline{P} sufficiently large so that they are not binding.

We simulate the OLFC-system as well as the swing dynamics (30) without load control ($d_i = 0$), after introducing a perturbation at bus 29 of $P_1^m = -2$ p.u.. Figures 3 and 4 show the evolution of the bus frequencies for the uncontrolled swing dynamics (a), the OLFC system without inter-area constraints (b), and the OLFC with area constraints (c).

It can be seen that while the swing dynamics alone fail to recover the nominal frequency, the OLFC controllers can jointly rebalance the power as well as recovering the nominal frequency. The convergence of OLFC seems to be similar or even better than the swing dynamics, as shown in Figures 3a and 3b, and Figures 4a and 4b.² Moreover, the inter-area constraints mitigates the propagation of the perturbation to Area 2 and makes convergence even faster.

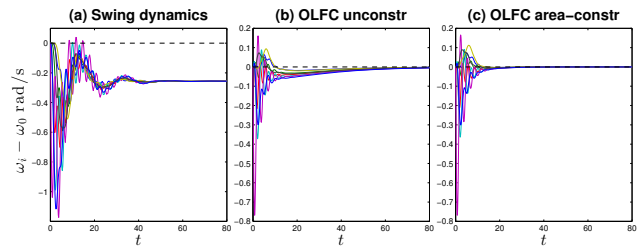


Fig. 3: Frequency evolution: Area 1

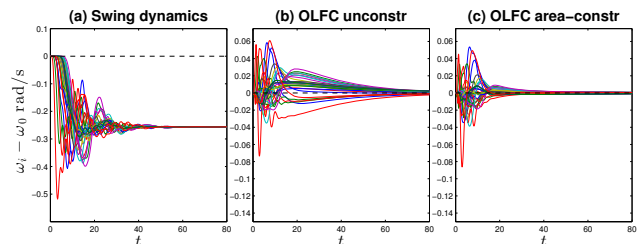


Fig. 4: Frequency evolution: Area 2

Finally, we illustrate the action of the thermal limit constraints by adding a constraint of $\bar{P}_e = 2.6$ p.u. and $\underline{P}_e = -2.6$ p.u. to the tie lines between areas. Figure 5 show the values of the multipliers λ_i , that correspond to the Locational Marginal Prices (LMPs), and the line flows of the tie lines for the OLFC with inter area flow constraints, but without thermal limits. It can be seen that neither the initial condition, nor the new steady state satisfy the our line limit. However, once we add thermal limits to our OLFC scheme in Figure 6 the system converges to a new operating point that satisfies our constraints.

²Notice the difference in the y axis scale.

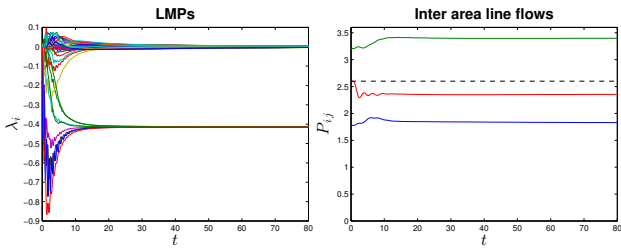


Fig. 5: LMPs and Tie Lines without Thermal Limits

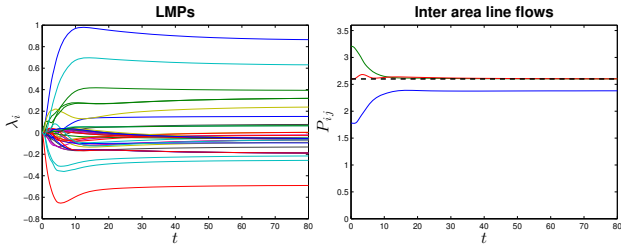


Fig. 6: LMPs and Tie Lines with Thermal Limits

VII. CONCLUDING REMARKS

This paper studies the problem of restoring the power balance and operational constraints of a power network after a disturbance by dynamically adapting the loads. We show that provided communication is allowed among neighboring buses, it is possible to rebalance the power mismatch, restore the nominal frequency, and maintain inter-area flow and thermal limits. Our distributed solution converges for every initial condition and numerical simulations are provided to verify our findings.

REFERENCES

- [1] A. J. Wood and B. F. Wollenberg, *Power Generation, Operation, and Control*, 2nd ed. John Wiley & Sons, Inc., 1996.
- [2] A. R. Bergen and V. Vittal, *Power Systems Analysis*, 2nd ed. Prentice Hall, 2000.
- [3] J. Machowski, J. Bialek, and J. Bumby, *Power system dynamics: Stability and Control*, 2nd ed. John Wiley & Sons, Inc., 2008.
- [4] M. D. Ilic, "From hierarchical to open access electric power systems," *Proceedings of the IEEE*, vol. 95, no. 5, pp. 1060–1084, 2007.
- [5] A. Kiani and A. Annaswamy, "A hierarchical transactive control architecture for renewables integration in Smart Grids," in *Decision and Control (CDC), 2012 IEEE 51st Annual Conference on*. IEEE, 2012, pp. 4985–4990.
- [6] F. C. Schweppe, R. D. Tabors, J. L. Kirtley, H. R. Outhred, F. H. Pickel, and A. J. Cox, "Homeostatic utility control," *IEEE Trans. Power App. Syst.*, vol. PAS-99, pp. 1151–1163, May/June 1980.
- [7] D. Trudnowski, M. Donnelly, and E. Lightner, "Power-system frequency and stability control using decentralized intelligent loads," in *Proc. of IEEE Transmission and Distribution Conf. Expo.*, Dallas, TX, USA, May 2006.
- [8] N. Lu and D. Hammerstrom, "Design considerations for frequency responsive grid friendly appliances," in *Proc. of IEEE Transmission and Distribution Conf. Expo.*, Dallas, TX, USA, May 2006.
- [9] J. Short, D. Infield, and F. Freris, "Stabilization of grid frequency through dynamic demand control," *IEEE Trans. Power Syst.*, vol. 22, no. 3, pp. 1284–1293, August 2007.
- [10] M. Donnelly, D. Harvey, R. Munson, and D. Trudnowski, "Frequency and stability control using decentralized intelligent loads: Benefits and pitfalls," in *Proc. of IEEE Power and Energy Society General Meeting*, Minneapolis, MN, USA, 2010, pp. 1–6.
- [11] A. Brooks, E. Lu, D. Reicher, C. Spirakis, and B. Wehl, "Demand dispatch," *IEEE Power and Energy Mag.*, vol. 8, no. 3, pp. 20–29, 2010.
- [12] D. S. Callaway and I. A. Hiskens, "Achieving controllability of electric loads," *Proceedings of the IEEE*, vol. 99, no. 1, pp. 184–199, 2011.
- [13] A. Molina-Garcia, F. Bouffard, and D. S. Kirschen, "Decentralized demand-side contribution to primary frequency control," *IEEE Trans. Power Syst.*, vol. 26, no. 1, pp. 411–419, 2011.
- [14] D. Hammerstrom, J. Brous, D. Chassin, G. Horst, R. Kajfasz, P. Michie, T. Oliver, T. Carlon, C. Eustis, O. Jarvegren, W. Marek, R. Munson, and R. Pratt, "Pacific Northwest GridWise testbed demonstration projects, part II: Grid Friendly Appliance project," Pacific Northwest Nat. Lab., Tech. Rep. PNNL-17079, October 2007.
- [15] M. Andreasson, D. V. Dimarogonas, H. Sandberg, and K. H. Johansson, "Distributed Control of Networked Dynamical Systems: Static Feedback, Integral Action and Consensus," *Automatic Control, IEEE Transactions on*, vol. 59, no. 7, pp. 1750–1764, Jul. 2014.
- [16] M. Andreasson, D. V. Dimarogonas, K. H. Johansson, and H. Sandberg, "Distributed vs. centralized power systems frequency control," in *Control Conference (ECC), 2013 European*, 2013, pp. 3524–3529.
- [17] X. Zhang and A. Papachristodoulou, "A real-time control framework for smart power networks with star topology," in *American Control Conference (ACC), 2013*, 2013, pp. 5062–5067.
- [18] Q. Shafiee, J. M. Guerrero, and J. C. Vasquez, "Distributed Secondary Control for Islanded Microgrids - A Novel Approach," *Power Electronics, IEEE Transactions on*, vol. 29, no. 2, pp. 1018–1031, Feb. 2014.
- [19] F. Dorfler and F. Bullo, "Breaking the hierarchy: Distributed control & economic optimality in microgrids," *arXiv.org*, 2014.
- [20] W. Liu, W. Gu, W. Sheng, X. Meng, Z. Wu, and W. Chen, "Decentralized Multi-Agent System-Based Cooperative Frequency Control for Autonomous Microgrids With Communication Constraints," *Sustainable Energy, IEEE Transactions on*, vol. 5, no. 2, pp. 446–456, 2014.
- [21] J. W. Simpson-Porco, F. Dorfler, F. Bullo, Q. Shafiee, and J. M. Guerrero, "Stability, power sharing, & distributed secondary control in droop-controlled microgrids distributed secondary control in droop-controlled microgrids," *2013 IEEE International Conference on Smart Grid Communications (SmartGridComm)*, pp. 672–677, 2013.
- [22] F. Dorfler, J. W. Simpson-Porco, and F. Bullo, "Plug-and-Play Control and Optimization in Microgrids," *motion.me.ucsb.edu*.
- [23] C. Zhao, U. Topcu, N. Li, and S. Low, "Design and Stability of Load-Side Primary Frequency Control in Power Systems," *Automatic Control, IEEE Transactions on*, vol. 59, no. 5, pp. 1177–1189, 2014.
- [24] N. Li, L. Chen, C. Zhao, and S. H. Low, "Connecting automatic generation control and economic dispatch from an optimization view," *American Control Conference*, 2014.
- [25] E. Mallada and S. H. Low, "Distributed frequency-preserving optimal load control," *IFAC World Congress*, 2014.
- [26] P. Kundur, *Power System Stability And Control*. McGraw-Hill, 1994.
- [27] Y.-H. Moon, B.-H. Cho, T.-H. Rho, and B.-K. Choi, "The development of equivalent system technique for deriving an energy function reflecting transfer conductances," *Power Systems, IEEE Transactions on*, vol. 14, no. 4, pp. 1335–1341, Nov. 1999.
- [28] C. Zhao, U. Topcu, N. Li, and S. H. Low, "Power system dynamics as primal-dual algorithm for optimal load control," *arXiv:1305.0585*, 2013.
- [29] S. P. Boyd and L. Vandenberghe, *Convex optimization*. Cambridge University Press, 2004.
- [30] F. P. Kelly, A. K. Maulloo, and D. K. Tan, "Rate control for communication networks: shadow prices, proportional fairness and stability," *Journal of the Operational Research society*, vol. 49, no. 3, pp. 237–252, 1998.
- [31] S. H. Low and D. E. Lapsley, "Optimization flow control i: basic algorithm and convergence," *IEEE/ACM Transactions on Networking (TON)*, vol. 7, no. 6, pp. 861–874, 1999.
- [32] R. Srikant, *The mathematics of Internet congestion control*. Springer, 2004.
- [33] D. P. Palomar and M. Chiang, "A tutorial on decomposition methods for network utility maximization," *Selected Areas in Communications, IEEE Journal on*, vol. 24, no. 8, pp. 1439–1451, 2006.
- [34] D. Feijer and F. Paganini, "Stability of primal–dual gradient dynamics and applications to network optimization," *Automatica*, vol. 46, no. 12, pp. 1974–1981, 2010.
- [35] A. Mas-Collel, M. D. Whinston, and J. Green, "Microeconomic theory," 1995.
- [36] H. K. Khalil, *Nonlinear systems*, 2nd ed. Prentice Hall, 2002.
- [37] J. H. Chow and K. W. Cheung, "A toolbox for power system dynamics and control engineering education and research," *Power Systems, IEEE Transactions on*, vol. 7, no. 4, pp. 1559–1564, 1992.